The Journal of Immunology

The Role of Phase II Antioxidant Enzymes in Protecting Memory T Cells from Spontaneous Apoptosis in Young and Old Mice

Hyon-Jeen Kim and Andre E. Nel

J Immunol 2005; 175:2948-2959; ;
doi: 10.4049/jimmunol.175.5.2948
http://www.jimmunol.org/content/175/5/2948

The Journal of Immunology is published twice each month by
The American Association of Immunologists, Inc.,
1451 Rockville Pike, Suite 650, Rockville, MD 20852

Print ISSN: 0022-1767 Online ISSN: 1550-6606.

The Role of Phase II Antioxidant Enzymes in Protecting Memory T Cells from Spontaneous Apoptosis in Young and Old Mice[1]

Hyon-Jeen Kim and Andre E. Nel[2]

Aging is associated with a functional decline and change in the phenotypic distribution of T cell subsets. The free radical theory of aging is widely promoted as the mechanistic basis for cellular senescence, including the immune system. Although the exact molecular explanation for the role of oxidative stress in cellular senescence is unclear, there is a connection to altered mitochondrial function, both as a contributor and as a target of oxidative stress. In this study we demonstrate that splenic T lymphocytes from old C57BL/6 mice exhibit a significant decline in mitochondrial membrane potential ($\Delta\psi_m$). However, despite this change, there is a lower rate of withdrawal apoptosis in the memory $CD4^+$ and $CD8^+$ T cells. To explain the survival of these long-lived cells against a background of increased oxidative stress, we demonstrate increased glutathione production and phase II enzyme expression, which combine to protect memory T cells against oxidative stress, mitochondrial dysfunction, and cell death. The accumulation of memory T cells with aging explains higher phase II enzyme expression in $CD4^+$ and $CD8^+$ T cells from old mice. Compared with wild-type mice, mice lacking the expression of *NF-E2-related factor-2*, the transcription factor that regulates phase II enzyme expression, had a significantly enhanced rate of apoptosis in the presence of an oxidative stress stimulus. *NF-E2-related factor-2*-deficient T cells exhibit a bigger decline in $\Delta\psi_m$ and increased reactive oxygen species production than cells from wild-type animals. Taken together, we suggest that phase II enzyme expression and the accompanying increase in intracellular thiol levels protect memory T cells from mitochondrial dysfunction and spontaneous apoptosis. ***The Journal of Immunology,*** **2005, 175: 2948–2959.**

Aging leads to a decline in the ability to mount a rigorous T cell response to newly encountered as well as recall Ags (1, 2). This decline manifests as a decrease in delayed-type hypersensitivity responses, diminished ability to respond to vaccination, and increased susceptibility to virulent viral and mycobacterial infections (1–4). This decline in cellular function occurs in parallel with changes in the T cell composition, cytokine production, altered ability of T cells to respond to TCR ligation, and altered regulation of programmed cell death (5–7). This includes a shift from a predominantly naive to a predominantly memory phenotype in rodents and humans (1, 8). This transformation is the result of ongoing immune challenge by infectious agents that promote T cell activation and the acquisition of a memory T cell phenotype (9). Due to homeostatic regulation that is aimed at keeping a constant T cell number, the slow accumulation of memory cells leaves "less space" for naive T cells (8). This leads to decline in the naive T cell numbers and lessens the ability of the elderly to respond to neo-Ags (8, 10).

These age-related changes in the immune system take place against the backdrop of increased levels of oxidative stress, which constitutes one of the key driving forces of aging (11). Although there are several potential sources of oxidative stress, the mitochondrion is of particular importance. This organelle develops cumulative problems with electron transport and proton pump activity during aging, leading to excessive production of reactive oxygen species (ROS)[3] (11–15). In addition to serving as a source for ROS production, mitochondria are targeted by oxygen radicals, leading to further interference in their function (16). Ultimately, this could impact cellular viability due to decreased ATP production as well as the release of proapoptotic factors that initiate caspase 9 activation (15, 16). An extensive literature details the changes in cellular survival and apoptosis with aging (17–20). However, the literature for T cells is confusing because evidence has been provided for both increased as well as decreased rates of programmed cell death (21–25). Although this apparent paradox could be due to the use of different stimuli and methods to assess apoptosis, it should be considered that memory and naive T cells exhibit different life spans and could be differently impacted by oxidative stress (21).

Oxidative stress refers to a state in which the production of ROS overwhelms the ability of antioxidant defense pathways to maintain redox equilibrium in the cell (26). Antioxidants are comprised of small and large molecules, among which glutathione (GSH) is representative of the low m.w. substances (26, 27). GSH is tripeptide that plays a role in ROS scavenging in addition to using its

Division of Clinical Immunology and Allergy, Department of Medicine, University of California, Los Angeles, CA 90095

Received for publication November 4, 2004. Accepted for publication June 6, 2005.

The costs of publication of this article were defrayed in part by the payment of page charges. This article must therefore be hereby marked *advertisement* in accordance with 18 U.S.C. Section 1734 solely to indicate this fact.

[1] This work was supported by U.S. Public Health Science National Institute of Aging Grant RO-1AG14992. The Center for AIDS Research Flow Cytometry Core Facility was supported by National Institutes of Health Grants CA16042 and AI28697 and by the Jonsson Comprehensive Cancer Center.

[2] Address correspondence and reprint requests to Dr. Andre E. Nel, Division of Clinical Immunology and Allergy, Department of Medicine, University of California, Los Angeles, CA 90095. E-mail address: anel@mednet.ucla.edu

[3] Abbreviations used in this paper: ROS, reactive oxygen species; 7-AAD, 7-aminoactinomycin D; ARE, antioxidant response element; CAT, catalase; $\Delta\Psi_m$, mitochondrial membrane potential; DEM, diethyl maleate; $DiOC_6$, 3,3′-dihexyloxabarbocyanine iodide; γ-GCLR, γ-glutamate cysteine ligase regulatory subunit; GPx, glutathione peroxidase; GR, glutathione reductase; GSH, glutathione; HE, hydroethidine; HO-1, heme oxygenase-1; MBB, monobromobimane; MFI, mean fluorescence intensity; NAC, *N*-acetylcysteine; Nrf2, NF-E2-related factor-2; NQO-1, NAD(P)H-quinone oxidoreductase-1; PI, propidium iodide; PTP, permeability transition pore; SFN, sulforaphane; SOD, superoxide dismutase.

0022-1767/05/$02.00

thiols to protect cysteine groups from oxidative damage (28). This includes protection of the vicinal thiol groups located in the mitochondrial permeability transition pore (PTP) (29). In the course of protecting against oxidative stress, GSH is converted to a dithiol derivative, such that a decline in the cellular GSH/GSH dithiol derivative ratio serves as a parameter for oxidative stress (28, 30). Large molecular antioxidants include classical antioxidant enzymes, such as superoxide dismutase (SOD), catalase (CAT), glutathione peroxidase (GPx), glutathione reductase (GR), and γ-glutamate cystein ligase (γ-GCL). Their activity is bolstered by the detoxification and antioxidant activity of GST and NADPH quinone oxidoreductase (NQO-1) as well as the enzyme responsible for heme catabolism, heme oxygenase 1 (HO-1) (26–28, 31). Collectively, these are known as phase II enzymes, which in addition to defense against oxidative stress, use a common transcription factor and gene expression pathway (31, 32). Transcriptional activation of phase II promoters requires occupancy of the antioxidant response element (ARE) by the basic region-leucine zipper transcription factor, NF-E2-related factor-2 (Nrf2) (31, 32). More recently, Nrf2 has also been shown to play a role in the regulation of cellular apoptosis (33).

In this communication we explore the roles of antioxidant enzymes and GSH in preventing programmed cell death and mitochondrial function in the memory and naive T cell subsets in young and old mice. This investigation was sparked by the observation that memory T cells exhibit a lower mitochondrial membrane potential ($\Delta\psi_m$) in aged mice, yet show a reduced rate of withdrawal apoptosis. We hypothesized that in order for memory T cells to protect themselves against a higher rate of oxidative stress and mitochondrial dysfunction during aging, these cells need a strengthened antioxidant defense. Our data demonstrate increased intracellular thiol levels and phase II enzyme expression in splenic T cells from old compared with young mice, especially in the $CD44^{high}$ T cell subsets. We demonstrate that Nrf2 plays a key role in initiating these protective responses, and that the deficiency of this transcription factor sensitizes memory T cells from younger animals to undergoing apoptosis and mitochondrial dysfunction in the presence of oxidative stress.

Materials and Methods

Mice

Male C57BL/6 (B6) mice were used in this study. Young (4-wk-old) mice were obtained from The Jackson Laboratory; old (18-mo-old) mice were purchased from the National Institute of Aging colony. These animals were killed at the ages of 2–4 and 19–21 mo, respectively, to compare the T cell responses in young and old mice. To study the role of Nrf2 regulation, 2- to 3-mo-old $Nrf2^{+/+}$ and $Nrf2^{-/-}$ mice were used. These animals, which were initially obtained from Dr. Y. Kan (University of California, San Francisco, CA) (34), were backcrossed onto a C57BL/6 background for six generations. Mice were housed at the Division of Laboratory Animal Medicine vivarium at the University of California at Los Angeles.

Reagents

RPMI 1640 and FCS were obtained from Mediatech and Irvine Scientific, respectively. Nylon wool fiber columns were obtained from Polysciences. The $CD4^+$ T cell isolation kit was purchased from Miltenyi Biotec. The Annexin V^{FITC} kit was obtained from Trevigen. Annexin V-allophycocyanin was obtained from BD Pharmingen, and 7-aminoactinomycin D (7-AAD) was purchased from Calbiochem. Monobromobimane (MBB), 3,3′-dihexyloxabarbocyanine iodide ($DiOC_6$), and hydroethidine (HE) were purchased from Molecular Probes. *N*-acetylcysteine (NAC) and sulforaphane (SFN) were obtained from Sigma-Aldrich. Abs used to stain cells for CD4, CD8α, and CD44 were obtained from BD Pharmingen. Anti-HO-1 mAb was purchased from Stressgen. Anti-β-actin mAb was obtained from Santa Cruz Biotechnology. Biotinylated swine anti-rabbit and rabbit anti-goat Abs were obtained from DakoCytomation. ECL reagents were purchased from Pierce. Primers for real-time PCR (see below) were purchased from E-Oligos. All organic solvents used were of Fisher Optima grade, and the solid chemicals were of analytical reagent grade.

Purification of T cells with nylon-wool columns

The spleens were aseptically removed for the preparation of a single-cell suspension. RBC were lysed with ammonium chloride. After washing with PBS and complete medium (see below), T cells were purified through the use of nylon-wool fiber columns, according to the manufacturer's recommendations. Briefly, columns were washed with complete medium and incubated at 37°C for 1 h. Each 4-ml column was loaded with splenocytes obtained from individual animals. After incubation at 37°C for 1 h, the nonadherent cells were eluted in a 30-ml wash. After additional washing, these cells were resuspended in complete medium, and their viability was assessed by trypan blue staining.

Cellular culture conditions and stimulation

Nylon wool-purified spleen T cells were resuspended in standard RPMI 1640 tissue culture medium supplemented with 10% FCS, 1% penicillin/streptomycin, and 1% glutamine at 10^6 cells/ml and subsequently cultured in 24-well plates for 1 day. For stimulation, cells were cultured in the presence of 20 mM NAC, 6 μM SFN, or 0.2 μM diethyl maleate (DEM). All cultures were conducted in 5% CO_2 in a humidified incubator at 37°C.

Magnetic bead separation of $CD4^+$ T cells and fluorescence sorting of $CD4^+/CD44^{low}$ and $CD4^+/CD44^{high}$ T cells

Magnetic cell sorting was performed as previously described (35). This involved negative $CD4^+$ enrichment by an isolation kit that depletes non-$CD4^+$ T cells according to the manufacturer's instructions. Briefly, the autoMACS (Miltenyi Biotec) system was used to separate unlabeled from labeled cells by the sequential addition of the biotin-Ab mixture and anti-biotin microbeads. After elution of the $CD4^+$ population, their purity was confirmed by flow cytometry. For purification of the respective $CD4^+/CD44^{low}$ and $CD4^+/CD44^{high}$ subsets, the negatively selected $CD4^+$ cell population was stained with FITC-conjugated anti-CD44 Ab (2 μg/10^7 cells) and PE-conjugated anti-CD4 Ab (2 μg/10^7 cells). After incubation in staining buffer (PBS, 2% FCS, and 0.1% sodium azide) at 4°C for 30 min in the dark, cells were washed and sorted in a FACSVantage fluorescence sorter (BD Biosciences). Aliquots of the fractionated $CD4^+/CD44^{low}$ and $CD4^+/CD44^{high}$ populations were counted and used for assessing their purity by flow cytometry.

Multicolor flow cytometry

Three-color flow cytometry to assess 7-AAD, $DiOC_6$, or MBB fluorescence in CD4/CD8 as well as $CD44^{high}/CD44^{low}$ subsets was performed as follows. Nylon wool purified splenic T cells (10^6) were initially stained with a combination of either PE-conjugated anti-CD4 or anti-CD8α Abs (0.2 μg) plus FITC- or PE-Cy5-conjugated anti-mouse CD44 Abs (0.2 μg) at 4°C in staining buffer for 30 min in the dark. After washing, cells were further stained with 7-AAD, $DiOC_6$, or MBB as described below. Samples were analyzed in an LSR flow cytometer (BD Biosciences) using the following excitation and emission settings: FITC, 488 and 530 nm (FL-1 channel); PE, 488 and 575 nm (FL-2 channel); and PE-Cy5, 488 and 670 nm (FL-3 channel). Multicolor flow cytometry to assess $DiOC_6$ and HE fluorescence in total T cells or CD4/CD8 and $CD44^{high}/CD44^{low}$ subsets was performed as follows. Cell staining with either PE-conjugated anti-CD4 or anti-CD8α Abs (0.2 μg) plus allophycocyanin-conjugated anti-mouse CD44 Abs (0.2 μg) was performed as described above, followed by the addition of $DiOC_6$ and HE as described below. Samples were analyzed in a FACSCalibur flow cytometer (BD Biosciences) using the following excitation and emission settings: $DiOC_6$, 488 and 530 nm (FL-1 channel); PE, 488 and 575 nm (FL-2 channel); HE, 488 and 670 nm (FL-3 channel); and allophycocyanin, 488 and 661 nm (FL-4 channel). For both protocols, a minimum of 20,000 events were collected and analyzed with Cell-Quest software. Forward and side scatters were used to gate out cellular fragments.

Detection of apoptosis by annexin V/propidium iodide (PI) staining

Nylon-wool-purified T cells (10^6/ml) were cultured for 1 day in complete medium. After washing in PBS, the cell pellets were resuspended in 100 μl of binding buffer containing 0.025 μg of annexin V-FITC and 4.75 μg of PI for 15 min at room temperature, according to the manufacturer's recommendations. Cells were immediately analyzed in a LSR flow cytometer. FITC-conjugated annexin V and PI were analyzed at an excitation setting of 488 nm, and the emissions were assessed at 530 nm (FL-1 channel) and

575 nm (FL-2 channel), respectively. To assess cell death in $DiOC_6$/HE-stained cells (see below), flow cytometry was performed by introducing 5 μl of annexin V-allophycocyanin to 10^5 cells in 100 μl of 1× binding buffer. After incubation at room temperature for 15 min in the dark, cells were analyzed in the FACSCalibur instrument. Annexin V-allophycocyanin fluorescence was assessed at excitation and emission settings of 488 and 661 nm (FL-4 channel), respectively.

Detection of apoptosis by 7-AAD staining

7-AAD is a fluorescent dye that intercalates into DNA and is useful for measuring apoptosis in lymphoid cells (36). Use of this protocol allows for the identification of live (7-AAD^{dull}), early apoptotic (7-AAD^{int}), and late apoptotic/necrotic (7-AAD^{bright}) cells (37–39). Briefly, nylon-wool-purified splenic T cells were cultured for 1 day in 1 ml of medium in 24-well plates. After staining with anti-CD4, anti-CD8α, and anti-CD44 Abs as described above, cells were washed in staining buffer and incubated with 10 μg/ml 7-AAD at 4°C for 20 min in the dark. Cells were immediately analyzed in a LSR flow cytometer, using excitation and emission settings of 488 and 670 nm (FL-3 channel), respectively.

Assessment of $\Delta\psi_m$ and ROS production

$\Delta\psi_m$ was quantified using $DiOC_6$, a positively charged fluorophore that accumulates in the mitochondrion. After staining of CD4/CD8α and CD44 as described above, cells were suspended in 1 ml of serum-free medium with 20 nM $DiOC_6$. After 30-min incubation at 37°C, the cells were analyzed in a LSR flow cytometer using excitation and emission wavelengths of 488 and 530 nm (FL-1 channel), respectively. This assessment was combined with staining for HE, a fluorophore that is converted to hydroethidium, mostly by superoxide. Dual $DiOC_6$/HE fluorescence was performed by including 1 μM HE in the incubation mixture for 30 min at 37°C. $DiOC_6$ and HE were analyzed in the FACSCalibur at an excitation setting of 488 nm, and the emissions were assessed at 530 nm (FL-1 channel) and 670 nm (FL-3 channel), respectively.

Measurement of intracellular thiols

Intracellular thiol levels in T cell subsets were measured using MBB (40, 41). Working solutions of MBB (1 mM) in PBS were made up freshly from a 40 mM MBB stock solution in DMSO (stored at −80°C). After surface staining for CD4/CD8α and CD44 as described above, T cells were resuspended in PBS at a concentration of 10^6 cells/ml. MBB was added to a final concentration of 40 μM and incubated at room temperature for 10 min. MBB fluorescence was excited by the UV laser tuned to 325 nm, and emission was measured at 510 nm (FL-4 channel) in the LSR flow cytometer.

RNA isolation from T cells

Total RNA was extracted from T cells using the Ultraspec RNA isolation system (Biotecx Laboratories) according to the manufacturer's recommendations. Contaminating DNA was removed using a DNA-free kit (Ambion). Total RNA was spectrophotometrically quantitated. A 1-μg RNA sample was reverse transcribed using the iScript cDNA Synthesis kit (Bio-Rad). The cDNA template was stored at −40°C.

Real-time RT-PCR to quantitate phase II enzyme and Nrf2 mRNA expression

PCR was conducted with an iQ SYBR Green Supermix (Bio-Rad) using an iCycler (Bio-Rad) according to the manufacturer's instructions. The primers, which were designed using the Primer3 website (⟨www-genome.wi.mit.edu/cgi-bin/primer/primer3_www.cgi⟩), are as follows (42): 1) HO-1, forward, 5′-CACGCATATACCCGCTACCT-3′, and reverse, 5′-CCAGAGTGTTCATTCGAGCA-3′; 2) NQO-1, forward, 5′-TTCTCTGGCCGATTCAGAGT-3′, and reverse, 5′-GGCTGCTTGGAGCAAAATAG-3′; 3) GPx, forward, 5′-GTCCACCGTGTATGCCTTCT-3′, and reverse, 5′-TCTGCAGATCGTTCATCTCG-3′; 4) γ-GCLR, forward, 5′-TGGAGCAGCTGTATCAGTGG-3′, and reverse, 5′-AGAGCAGTTCTTTCGGGTCA-3′; 5) CAT, forward, 5′-GAGACCTGGGCAATGTGACT-3′; reverse, 5′-GTTTACTGCGCAATCCCAAT-3′; 6) β-actin, forward, 5′-AGCCATGTACGTAGCCATCC-3′, and reverse, 5′-CTCTCAGCTGTGGTGGTGAA-3′; and 7) Nrf2, forward, 5′-CTCGCTGGAAAAAGAAGTGG-3′, and reverse, 3′-CCGTCCAGGAGTTCAGAGAG-5′. The final PCR mixture contained 1 μl of cDNA template and 400 nM of the forward and reverse primers in a final volume of 25 μl. Samples were run concurrently with standard curves derived from PCR products, and serial dilutions were performed to obtain appropriate template concentrations. β-Actin was used as a reference gene for the recovery of RNA as well as RT efficiency. Melting curve analysis was used to confirm specific replicon formation.

Western blotting

Whole T cell lysates were used to perform immunoblotting as described previously (43). The protein concentration was determined using the Bradford method. One hundred fifty micrograms of total protein was separated by SDS-PAGE before transfer to polyvinylidene difluoride membranes. HO-1 protein was detected by anti-HO-1 mAb at 0.3 μg/ml and rabbit anti-mouse Ab conjugated to HRP according to the manufacturer's instructions. Anti-β-actin Ab was used at 1 μg/ml. Biotinylated swine anti-rabbit Ab (1/1,000) was used as secondary Ab, followed by HRP-conjugated avidin-biotin complex (1/10,000). Blots were developed with the ECL reagent according to the manufacturer's instruction.

Statistical analysis

Results were expressed as the mean ± SD and analyzed by Student's *t* test. All differences of $p < 0.05$ were considered significant.

Results

Aging is associated with a lower rate of spontaneous apoptosis in the memory T cell subset in C57BL/6 mice

Although aging is associated with a change in T cell survival, it is still controversial whether this amounts to increased or decreased rates of apoptosis (21, 22). The use of annexin V/PI staining to evaluate spontaneous apoptosis in T cells, 1 day after the removal of spleens of young (2–4 mo) and old (19–21 mo) mice, revealed a significant increase in the percentage of live (annexin V^-/PI^-) and a significant decrease in the percentage of apoptotic (annexin V^+/PI^+) cells from old mice (Fig. 1). This difference remained statistically different over an observation period of up to 3 days, at which stage the rate of apoptosis in young T cells approached 100% (data not shown).

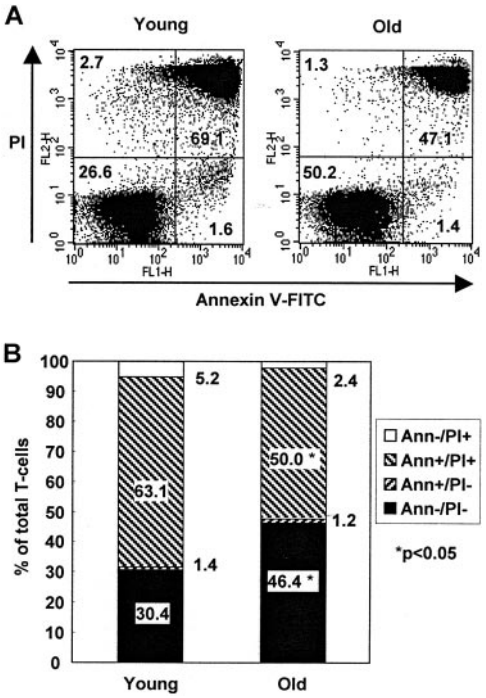

FIGURE 1. Age-dependent differences in spontaneous apoptosis as determined by annexin V/PI staining. Nylon wool-purified T cells from young and old mice ($n = 4$ each) were cultured ex vivo for 1 day, then prepared for flow cytometry as described in *Materials and Methods*. *A*, Representative annexin V-FITC/PI profile from a young and an old animal. The number in each quadrant refers to the percentage of cells in each population. *B*, Flow data, expressed as a stack diagram. The data represent the mean percentage of cells in each quadrant for all four animals in each age group. The SD varied <10% for each data point. The experiment was repeated three times. *, $p < 0.05$, young compared with old.

Another approach to assessing apoptosis in T cell subsets is the use of 7-AAD staining in combination with fluorescent Abs to CD4, CD8α, and anti-CD44. When using a dual-color flow cytometry protocol to assess cellular viability in unfractionated $CD4^+$ and $CD8^+$ T cells, we found a significant increase in the percentage of live (7-AAD^{dull}) cells in old compared with young T cell subsets (Fig. 2*A*). At the same time, there was a statistically significant decrease in the percentage of 7-AAD^{int} and 7-AAD^{bright} cells in old compared with young animals (Fig. 2*B*). These represent early and late apoptotic cells, respectively (37–39).

When using a three-color approach to assess the rates of cell death in $CD44^{high}$ and $CD44^{low}$ T cell subsets, we observed even greater differences between young and old animals (Fig. 2*C*). We found a statistically significant increase in the rate of cell death in $CD44^{high}$ T cells from young compared with old animals in both $CD4^+$ and $CD8^+$ subsets (Fig. 2*C*). The same was true for the $CD8^+/CD44^{low}$, but not the $CD4^+/CD44^{low}$, subset (Fig. 2*C*).

Taken together, these results show that T cells from old mice have an increased resistance to spontaneous apoptosis compared with those from young mice. This difference is especially noticeable in $CD44^{high}$ subsets. A likely explanation for triggering spontaneous cell death is cytokine or growth factor withdrawal. This idea is supported by a significant drop in the rate of apoptosis in $CD8^+$ T cells by the inclusion of IL-15 in the culture medium (data not shown). Although CD44 expression was increased in some effector T cell subsets, for the purposes of this communication, we will refer to the $CD44^{high}$ and $CD44^{low}$ subsets as memory and naive T cells, respectively.

Aging is associated with decreased $\Delta\psi_m$ in T cells from old mice

Growth factor withdrawal apoptosis is known to impact mitochondrial pathways that regulate lymphocyte and thymocyte viability (44–46). Growth factor withdrawal also perturbs signaling pathways that regulate the open-closed status of the mitochondrial PTP (46). In case of large-scale PTP transition, this can lead to the release of proapoptotic factors, dissipation of the $\Delta\psi_m$, and ROS generation (16). Aging exerts more subtle effects on the mitochondrion, including interference in inner membrane electron transduction, ROS generation, and effects on the threshold for PTP transition (16). To explore differences in the $\Delta\psi_m$ in splenic T cells from young and old animals, the fluorochrome, $DiOC_6$, was used in combination with fluorescent anti-CD44 and anti-CD4/CD8α Abs. A representative experiment is shown in Fig. 3*A*, which demonstrates a decreased $\Delta\psi_m$ in T cells from old compared with young mice. This difference holds true in the $CD4^+$ and $CD8^+$ subsets (Fig. 3*A*). When comparing the mean fluorescence intensity (MFI) for $DiOC_6$ in the total T cell population as well as the $CD4^+$ and $CD8^+$ subsets, there was a statistically significant decline in old compared with young ($n = 4$) animals (Fig. 3*B*). Additional breakdown into $CD44^{high}$ and $CD44^{low}$ cells showed that aging had a greater effect on the $CD44^{high}$ than the $CD44^{low}$ subset (Fig. 3*C*).

One of the key theories of aging is that mitochondrial dysfunction and ROS production are responsible for cellular senescence (11, 15). To assess ROS production concomitant with $\Delta\psi_m$, we used dual-color $DiOC_6$/HE staining (47). HE is converted to a hydroethidium by ROS, particularly O_2^-. This delineated three phenotypically different populations: $DiOC_6^{high}$/HE^{low}-, $DiOC_6^{low}$/HE^{low}-, and $DiOC_6^{low}HE^{high}$-stained cells (Fig. 4*A*) (47). When comparing the $CD4^+$ subsets from young and old animals, the cells from old animals exhibited a statistically significant increase in the percentage of $DiOC_6^{low}/HE^{low}$ cells (Fig. 4*A*). Additional breakdown into $CD4^+/CD44^{high}$ and $CD4^+/CD44^{low}$ subsets showed that the $DiOC_6^{low}/HE^{low}$ phenotype was significantly increased in the memory and naive populations of old mice (Fig. 4*A*, *middle* and *lower panels*). In

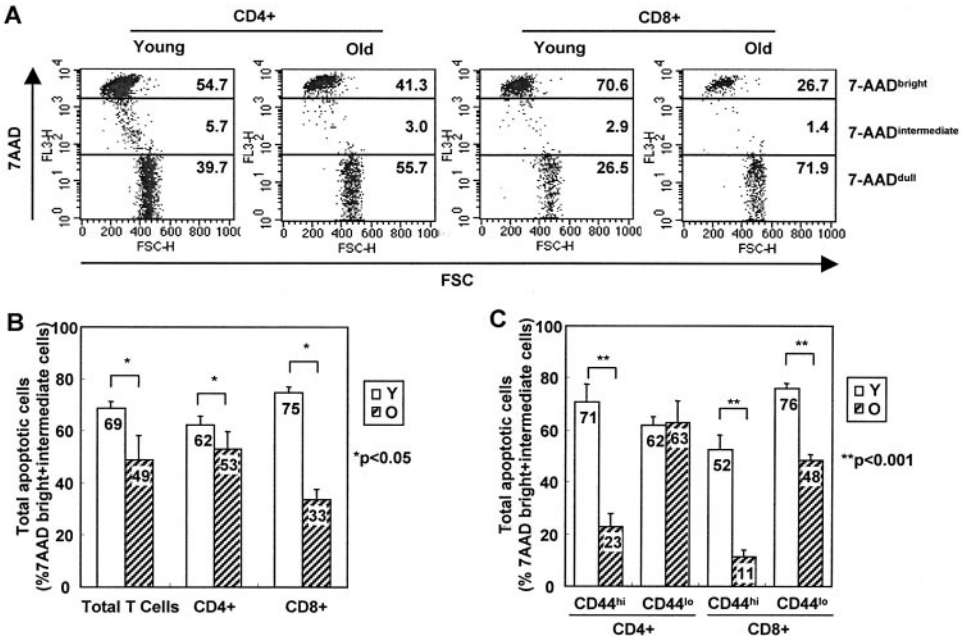

FIGURE 2. Spontaneous apoptosis of T cell subsets as determined by a 7-AAD assay. Nylon-wool-purified T cells from young and old mice were cultured ex vivo for 1 day. The cells were triple stained with PE-conjugated anti-CD4 or CD8α Abs, FITC-conjugated anti-CD44 Abs, and 7-AAD. *A*, Representative 7-AAD staining profile for $CD4^+$ and $CD8^+$ subsets in a young and an old mouse. Scattergrams were generated by combining forward light scatter (FSC) with 7-AAD fluorescence. Live, early, and late apoptotic cells were defined according to the level of 7-AAD staining, as indicated. Numbers refer to the percentage of cells in each category. *B*, Comparison of the percentage (mean ± SD) of total (early and late) apoptotic cells for young and old mice ($n = 4$/group). *C*, Comparison of the percentage (mean ± SD) of total apoptotic cells in the $CD4^+/CD44^{high}$, $CD4^+/CD44^{low}$, $CD8^+/CD44^{high}$, and $CD8^+/CD44^{low}$ subsets in young and old mice ($n = 4$/group). The experiment was repeated three times. *, $p < 0.05$; **, $p < 0.001$ (young compared with old).

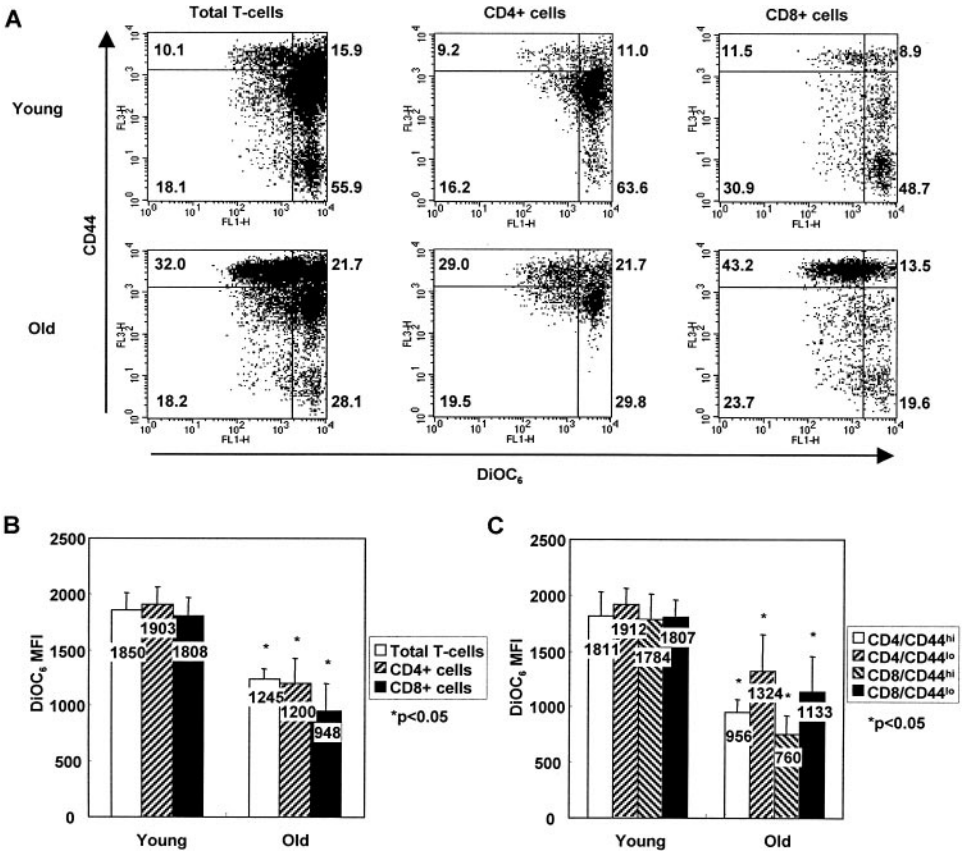

FIGURE 3. Age-dependent differences in $\Delta\psi_m$ in total and T cell subsets. Freshly isolated T cells were stained for either CD4 or CD8α, CD44, and $DiOC_6$ as described in *Materials and Methods*. *A*, Representative scattergram comparing total T cells and $CD4^+$ and $CD8^+$ subsets in a young and an old animal. The numbers refer to the percentage of cells in each population. *B* and *C*, MFI calculation for $DiOC_6$ (mean ± SD) for four animals in each age group. The experiment was repeated three times. *, $p < 0.05$, young compared with old.

contrast, the percentage of $DiOC_6^{low}/HE^{high}$ cells was significantly increased in the memory subset from young compared with old animals ($p < 0.01$; Fig. 4*A*, *middle panel*). Alternatively, if the number of $DiOC_6^{low}/HE^{high}$ cells was expressed as a percentage of the total T cells with a low $\Delta\psi_m$, there was a statistically significant increase in these ROS-producing cells in the $CD4^+$ as well as the corresponding $CD4^+/CD44^{high}$ and $CD4^+/CD44^{low}$ subsets in young animals (Fig. 4*B*). Similar data were obtained for the $CD8^+$ population (data not shown).

The $DiOC_6^{high}/HE^{low}$, $DiOC_6^{low}/HE^{low}$, and $DiOC_6^{low}HE^{high}$ populations each represent a different state of cellular viability, mitochondrial function, and ROS generation (47). Thus, the $DiOC_6^{high}/HE^{low}$ population has been depicted as viable cells with normal $\Delta\psi_m$ and negligible O_2^- production (47). Using dexamethasone as a stimulus, Zamzami et al. (47) provided evidence that the $DiOC_6^{low}HE^{low}$ population represents viable cells with reversible mitochondrial dysfunction and negligible O_2^- production, whereas the $DiOC_6^{low}HE^{high}$ population represents apoptotic cells with irreversible mitochondrial damage and O_2^- production. To demonstrate that this also holds true for splenic T cells undergoing withdrawal apoptosis, we used annexin V staining to demonstrate that the $DiOC_6^{low}HE^{high}$ phenotype includes mostly annexin V-positive cells, whereas the $DiOC_6^{high}/HE^{low}$ and $DiOC_6^{low}/HE^{low}$ populations include mostly annexin V-negative cells (Fig. 4*C*). These data are in agreement with the higher rates of spontaneous apoptosis in T cells from young animals (Figs. 1 and 2).

Evidence for altered GSH levels in T cells from young vs old mice

MBB reacts nonenzymatically with intracellular thiols to form a fluorescent compound that can be assessed by flow cytometry (41). Because GSH is the most abundant intracellular thiol source, MBB fluorescence intensity closely mirrors the GSH content of mammalian cells (41). A representative MBB staining profile for $CD4^+$ splenic T cells is shown in Fig. 5*A* (*left panel*). If further dissected to discern the contributions of $CD44^{high}$ and $CD44^{low}$ subsets, memory $CD4^+$ T cells show more intense MBB fluorescence than naive $CD4^+$ cells (Fig. 5*A*, *right panel*). Using MFI to compare young and old T cells, we observed a statistically significant increase in the intracellular thiol levels in old animals (Fig. 5*B*). This was true for total T cells as well as the $CD4^+$ and $CD8^+$ subsets (Fig. 5*B*). The aging effect was especially pronounced in the $CD4^+/CD44^{high}$ and $CD8^+/CD44^{high}$ subsets, but did not impact the $CD4^+/CD44^{low}$ and $CD8^+/CD44^{low}$ subsets (Fig. 5*C*). The data in Fig. 5*C* also show that memory T cells have a higher intracellular thiol content than naive T cells subsets regardless of age (Fig. 5*C*). This suggests that memory T cells have an increased capacity to defend themselves against antioxidant defense. This trend toward a higher GSH content is accentuated during aging.

Increased phase II mRNA expression in T cells from older animals

Intracellular GSH levels are regulated by a number of metabolic processes, including enzymes that regulate the synthesis, breakdown, and conjugation of GSH. These include the γ-GCLR regulatory subunit, GST, and GPx (48–50). The expression of these enzymes is dependent on transcriptional activation of an ARE in their promoters by the region-leucine basic zipper transcription factor, Nrf2 (31). Nrf2 also contributes to the expression of HO-1, CAT, and NQO-1 (31, 51, 52). Collectively, these phase II enzymes are responsible for GSH synthesis, ROS scavenging, and conjugation of pro-oxidative chemicals (31, 32). To determine whether the increase in GSH content is accompanied by increased phase II enzyme expression, we performed a quantitative real-time PCR analysis of T cells from young and old mice. The mRNA expression profiles for HO-1, NQO-1, GPx, γ-GCLR, and CAT are shown in Fig. 6*A*. These demonstrate that old mice had a statistically significantly increase in HO-1, NQO-1, and GPx mRNA

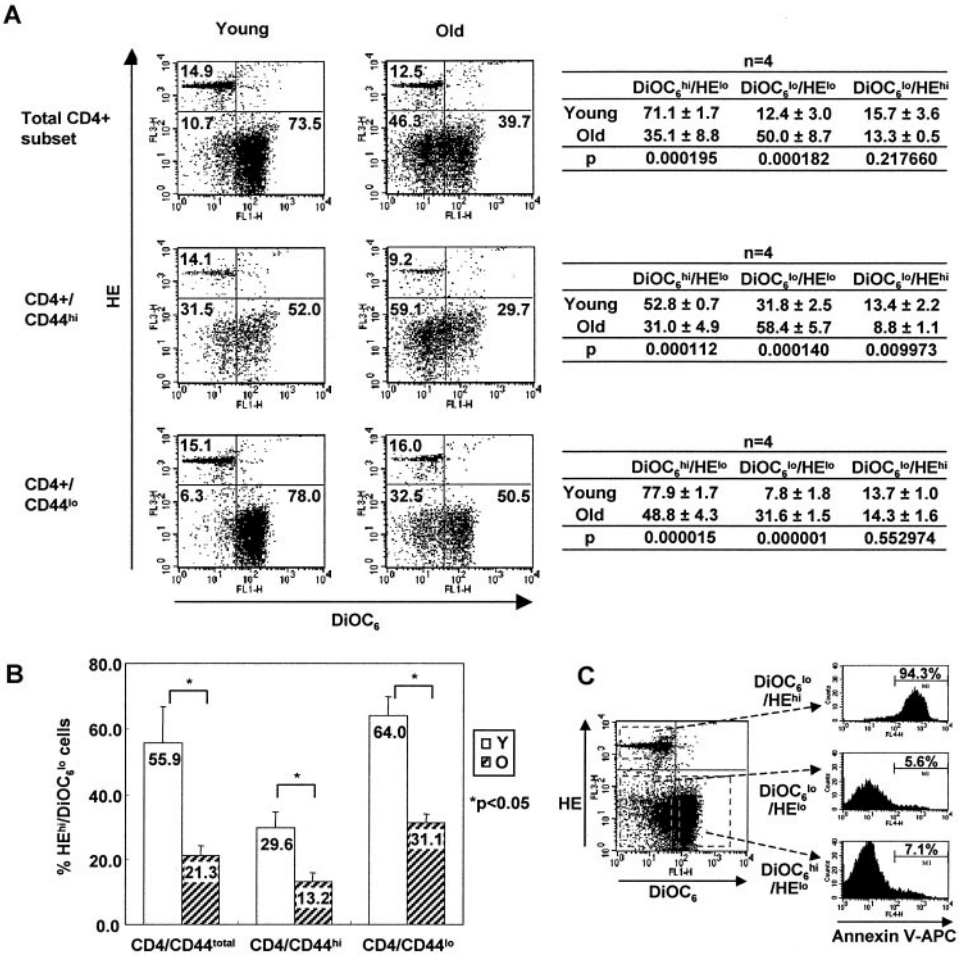

FIGURE 4. Comparison of $\Delta\psi_m$ and ROS production in T cell subsets from young and old animals by $DiOC_6$/HE staining. *A*, Freshly isolated T cells from four young and four old mice were stained with PE-conjugated anti-CD4 and anti-CD44 Abs, $DiOC_6$, and HE as described in *Materials and Methods*. The *left panel* shows a representative scattergram for the total $CD4^+$ as well as the $CD4^+/CD44^{high}$ and $CD4^+/CD44^{low}$ subsets in a young and an old animal. Definition of quadrants: LL, $DiOC_6^{low}/HE^{low}$; UL, $DiOC_6^{low}/HE^{high}$; LR, $DiOC_6^{high}HE^{low}$. The number in each quadrant refers to the percentage of cells in that population. The *right panel* shows the corresponding percentage (mean ± SD) of cells in each quadrant for the four animals in each age group. *B*, The graph shows the percentage HE^{high} cells among T cells with a decreased $\Delta\psi_m$ in the total $CD4^+$ as well as the $CD4^+/CD44^{high}$ and $CD4^+/CD44^{low}$ subsets in a young and an old animal. *, $p < 0.05$. *C*, Three-color flow cytometry for $DiOC_6$, HE, and annexin V-allophycocyanin staining. Histograms reflecting the percentage of annexin V-positive cells in each quadrant are shown.

expression, but did not show a significant change in γ-GCLR and CAT mRNA expression levels. The increase in HO-1 mRNA was accompanied by increased HO-1 protein levels in T cells from old compared with young animals (Fig. 6*B*). We also explored whether treatment with SFN, which induces Nrf2 release to the nucleus, will lead to quantitatively different responses in T cells from young and old animals. Splenic T cells were cultured in the presence of SFN for 1 day, and HO-1 mRNA expression was determined by RT-PCR (Fig. 6*C*). This electrophilic chemical induced statistically significant increases in HO-1 mRNA expression in young as well as old animals, with a bigger response differential in the latter age group (Fig. 6*C*).

To determine whether similar findings hold true in the $CD4^+$ subset, a negatively selected $CD4^+$ population was used for RNA extraction and real-time PCR analysis (35). This demonstrated a phase II expression profile very similar to that of the entire T cell population (Fig. 6, *A* and *D*). Thus, the messages for HO-1, NQO-1, and GPx, but not γ-GCLR and CAT, were increased in $CD4^+$ T cells from old compared with young animals (Fig. 6*D*).

The negatively selected $CD4^+$ cells were further subfractionated into $CD44^{high}$ and $CD44^{low}$ subsets by fluorescence sorting. This yielded $CD4^+/CD44^{high}$ and $CD4^+/CD44^{low}$ populations that were >98% pure as demonstrated by two-color flow cytometry (Fig. 7*A*). RT-PCR analysis showed that memory T cells express significantly more HO-1, NQO-1, GPx, and CAT mRNA levels than naive T cells regardless of age (Fig. 7*B*). Although γ-GCLR was significantly increased in memory T cells from young animals, this increase was not statistically significant in old animals (Fig. 7*B*). Although the relative mRNA expression levels were not significantly different in old vs young animals, memory T cell accumulation with aging led to increased phase II enzyme expression in the total T cell population as well as the $CD4^+$ subset in old animals (Fig. 6, *A* and *D*)

Increased Nrf2 mRNA expression in memory $CD4^+$ T cells

Nrf2 plays an important role in phase II enzyme expression and cellular defense against oxidative stress (31). Moreover, through its regulation of antioxidant defense, Nrf2 also regulates apoptosis induction by death receptors (53). Under basal conditions, Nrf2 is sequestered in the cytosol by a chaperone, Keap I, which is responsible for the shuttling of this transcription factor to the 26S proteosome (54, 55). This leads to continuous Nrf2 degradation and a short half-life (54, 55). Under oxidative stress conditions, Nrf2 is released from Keap I, leading to its escape from proteolytic degradation (42). This leads to Nrf2 accumulation in the nucleus and transcriptional activation of the ARE (42, 54, 55). In addition to the regulation of Nrf2 abundance by proteosomal degradation, this transcription factor autoregulates its own gene via the ARE in its promoter (56, 57). A comparison of *Nrf2* mRNA levels in $CD44^{high}$ and $CD44^{low}$ T cells showed a significant increase in the former compared with naive cells regardless of age (Fig. 7*C*). However, relative expression levels did not change in either subset with aging (Fig. 7*C*).

Evidence that Nrf2 influences spontaneous apoptosis by regulating the GSH content of T cells

In Figs. 1, 2, and 5, we have demonstrated that T cells from old mice exhibit a reduced rate of spontaneous apoptosis coupled with

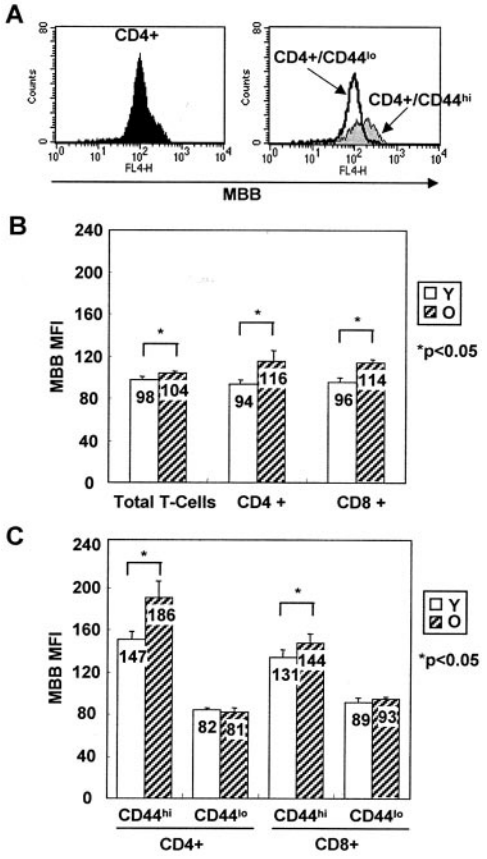

FIGURE 5. Assessment of intracellular thiol levels in T cells using MBB staining and flow cytometry. Nylon-wool-purified T cells were stained with Abs to CD4 or CD8α, and CD44. Cells were stained with 40 μM MBB as described in *Materials and Methods*. *A*, The histogram shows a representative analysis of $CD4^+$, $CD4^+/CD44^{high}$, and $CD4^+/CD44^{low}$ cells from a randomly chosen old animal. *B* and *C*, MBB staining of total T cells and $CD44^{high}/CD44^{low}$ subsets comparing MFI in four young and four old animals. Results are the mean $\pm$ SD. The experiment was repeated three times. $*$, $p < 0.05$.

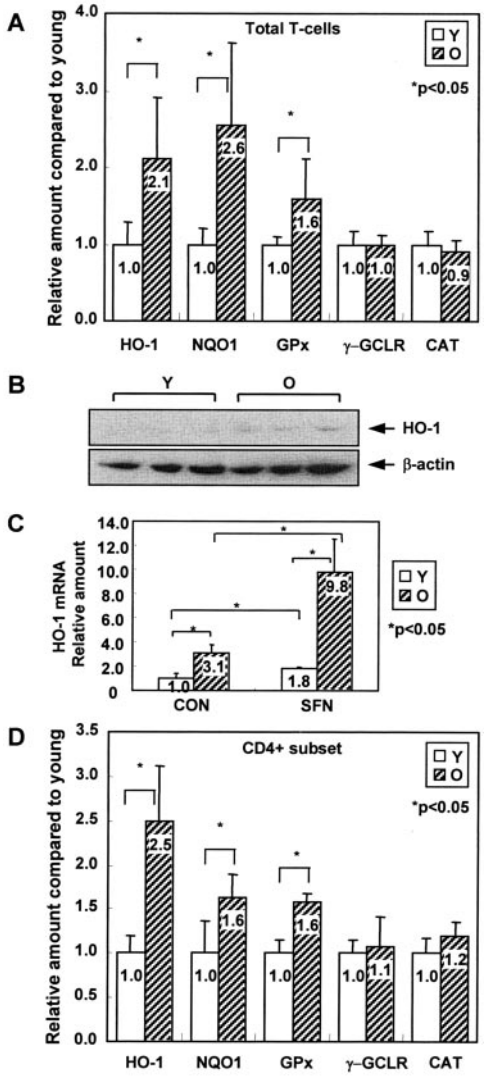

FIGURE 6. Real-time PCR analysis and immunoblotting to compare phase II enzyme gene expression in young and old animals. *A*, Total RNA was extracted from nylon-wool column-purified spleen T cells and used to conduct real-time PCR for HO-1, NQO-1, GPx, γ-GCLR, and CAT expression as described in *Materials and Methods*. β-Actin was used as a reference gene. Results represent the fold increase (mean $\pm$ SD) of old compared with young mice ($n = 4$). $*$, $p < 0.05$. *B*, Immunoblotting for HO-1 protein expression in the whole cell lysate of total T cells from young and old mice. Each lane is representative of three young and three old mice. *C*, Splenic T cells from four young and four old mice were treated with 6 μM SFN for 1 day, then subjected to real-time PCR analysis for HO-1 expression. Results represent the fold difference (mean $\pm$ SD) compared with the unitary value of untreated young mice ($n = 4$). $*$, $p < 0.05$, young vs old, or SFN vs control mice. *D*, Phase II enzyme mRNA expression in $CD4^+$ T cells from young and old animals. β-Actin was used as a reference gene. Results represent the fold increase (mean $\pm$ SD) of old compared with young mice ($n = 4$). $*$, $p < 0.05$.

an increase in thiol levels. Furthermore, memory cells showed higher GSH levels (Fig. 5) and a decreased rate of spontaneous apoptosis compared with naive cells (Figs. 1 and 2). We asked, therefore, whether an increase in GSH levels affects spontaneous apoptosis. NAC is a thiol antioxidant that serves as a GSH precursor (58). Our data show that the increase in MBB staining (Fig. 8*A*) during NAC treatment is accompanied by a significant decrease in the rate of cell death in young as well as old animals (Fig. 8*B*). These data support the idea that increased intracellular thiol levels protect against withdrawal apoptosis.

To provide proof-of-principle evidence that Nrf2 is involved in T cell apoptosis under conditions of oxidative stress, splenic T lymphocytes were purified from wild-type ($Nrf2^{+/+}$) and *Nrf2*-deficient ($Nrf2^{-/-}$) mice (34) and incubated in the presence of DEM, a chemical that depletes GSH. Apoptosis was assessed 24 h later by 7-AAD staining. No significant change in the rate of apoptosis was seen under basal conditions. However, DEM induced more cell death in $Nrf2^{-/-}$ compared with wild-type T cells (Fig. 9*A*). DEM treatment also induced a more precipitous decline in intracellular thiol (MBB) levels in $Nrf2^{-/-}$ compared with wild-type animals (data not shown). These results indicate that Nrf2 plays a role in controlling cell viability, and that knockout of this transcription factor leads to an increased rate of cell death under conditions of oxidative stress. Unfortunately, we did not have aged $Nrf2^{-/-}$ mice to study the effects of aging in that setting.

To relate the onset of apoptosis to mitochondrial perturbation, we used $DiOC_6$/HE staining to examine freshly isolated T cells from wild-type and *Nrf2*-deficient animals (Fig. 9, *B* and *C*). This yielded the same phenotypes as those described in Fig. 4 (Fig. 9*B*). Under basal conditions, there was a significant increase in the percentage of $DiOC_6^{low}/HE^{high}$ cells in $Nrf2^{-/-}$ compared with $Nrf2^{+/+}$ mice (Fig. 9, *B* and *C*). Additional analysis of the effects

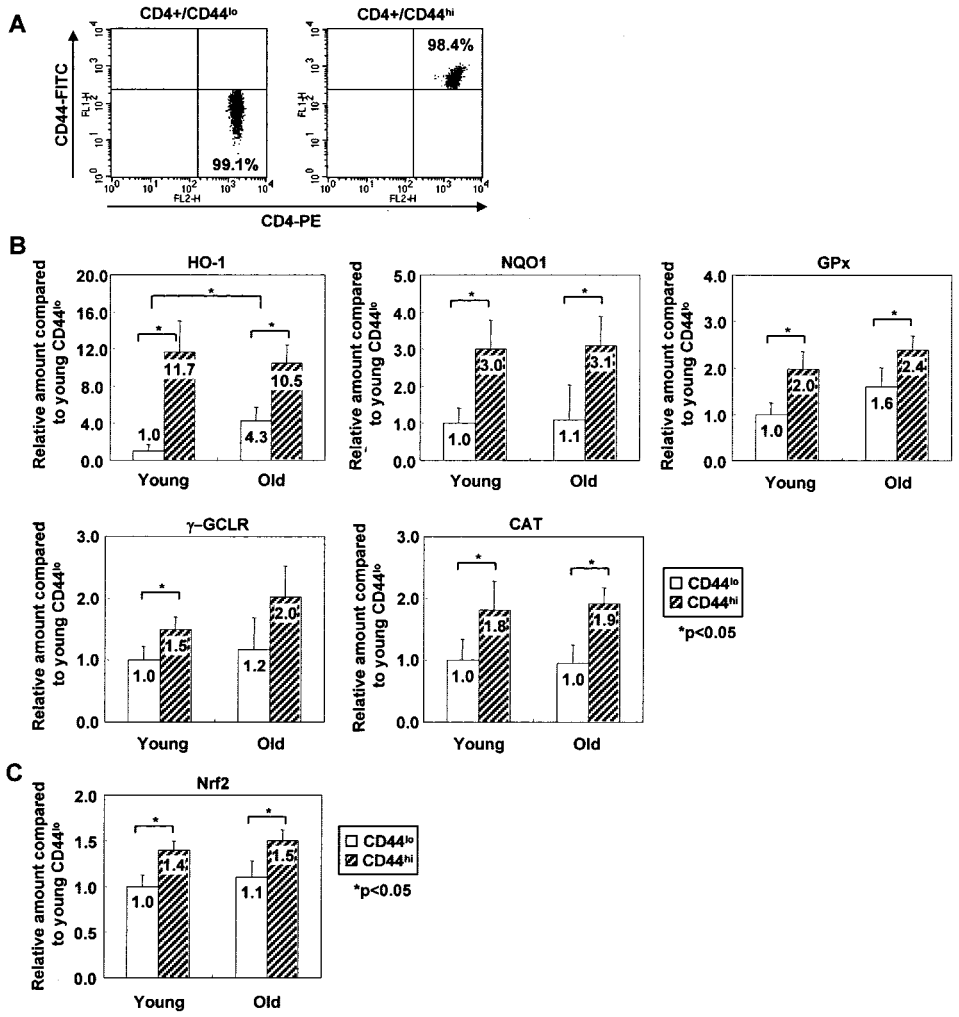

FIGURE 7. Phase II enzyme and *Nrf2* mRNA expression in the memory and naive $CD4^+$ subsets. *A*, Purity of the $CD4^+/CD44^{low}$ and $CD4^+/CD44^{high}$ subsets as determined by dual-color staining. *B* and *C*, Real-time PCR for HO-1, NQO-1, GPx, γ-GCLR, CAT, and *Nrf2* mRNA expression in memory ($CD4^+/CD44^{high}$) and naive ($CD4^+/CD44^{low}$) T cells of young and old mice. Data are expressed as the fold difference (mean ± SD) compared with the unitary value of the $CD44^{low}$ subset of young mice ($n = 4$). β-Actin was used as a reference gene. *, $p < 0.05$, naive vs memory, or young vs old mice.

of an oxidative chemical showed a dramatic increase in the percentage of $DiOC_6^{low}HE^{high}$ cells in T cells from *Nrf2*-deficient mice (Fig. 9*D*). Thus, DEM treatment induced >94% $DiOC_6^{low}HE^{high}$ cells in T cells from $Nrf2^{-/-}$ mice (Fig. 9*E*). This increase was significantly higher than the changes in T cells from wild-type mice (Fig. 9*E*). These results show that mice lacking *Nrf2* expression are more vulnerable to mitochondrial perturbation in the presence of an oxidative stimulus.

Discussion

We demonstrate that aging is associated with a decreased rate of spontaneous apoptosis and a decline in $\Delta\Psi_m$ in splenic T lymphocytes. These events are accompanied by increased phase II enzyme expression and GSH synthesis in T cells from aged mice. These changes were more prominent in the long-lived memory T cells, which demonstrate more severe mitochondrial dysfunction. Compared with wild-type mice, mice deficient in *Nrf2* expression had a significantly increased rate of apoptosis in response to oxidative stress stimuli. *Nrf2*-deficient T cells also showed a decreased $\Delta\Psi_m$ and increased ROS generation during DEM treatment. Taken together, these data show that Nrf2-mediated phase II enzyme expression and regulation of intracellular thiol levels protect cells against oxidative stress, mitochondrial dysfunction, and programmed cell death. This defense pathway is particularly important for the survival of memory T cells, which accumulate during aging.

The free radical theory of aging is widely accepted as a possible explanation for cellular senescence, including in the immune system (11–13). Various studies have shown that increased free radical production and oxidative modification of biologically important molecules play roles in cellular dysfunction and age-related disease phenomena (11, 12). Oxidative stress is a recognized initiator of programmed cell death, including regulation of T cell apoptosis under physiological and pathophysiological conditions (59–66). For instance, there are extensive data showing that oxidative stress plays a role in HIV pathology, including apoptosis and depletion of $CD4^+$ lymphocytes (59–64). Moreover, there is a strong association between decreased survival in HIV-infected subjects and low thiol levels in serum and $CD4^+$ cell (65, 66). A recent study by De Rosa et al. (59) showed that NAC therapy replenishes whole blood and T cell GSH levels in HIV-infected individuals, suggesting a possible therapeutic role in AIDS. Because apoptosis is a key protective mechanism against the accumulation of activated and effete T cells, interference in cell death by an up-regulated antioxidant defense could contribute to memory T cell retention during aging. Caloric restriction, the only established experimental antiaging paradigm, delays these phenotypic changes and the accompanying decline in immune function (10, 67, 68). Reduced calorie intake also leads to a reduction in free radical generation in mitochondria (69). Accordingly, caloric restriction reverses mitochondrial dysfunction (70, 71) and cellular apoptosis (72).

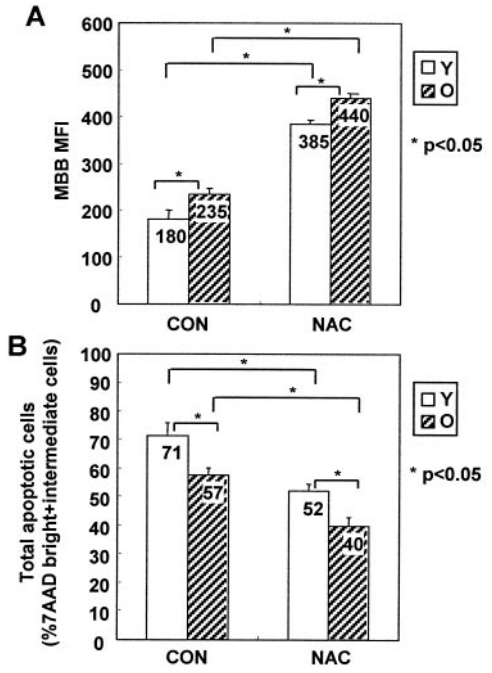

FIGURE 8. NAC protects against withdrawal apoptosis in T cells. Nylon-wool-purified T cells from young and old mice were cultured for 1 day in the absence or the presence of 20 mM NAC. The cells were stained with MBB or 7-AAD, followed by flow cytometric analysis. *A*, MBB staining intensity to show the change in intracellular thiol levels in young vs old mice. Data represent the mean ± SD for the MFI ($n = 4$). *B*, Comparison of the total (early plus late) apoptotic T cells in young and old mice. Data are expressed as the mean ± SD of the percentage total apoptotic cells ($n = 4$). The experiment was repeated three times. *, $p < 0.05$, young vs old, or NAC vs control mice.

Oxidative stress does not automatically lead to tissue injury, but elicits protective responses that are important for cellular maintenance, e.g., antioxidant defense and activation of cellular signal transduction pathways (73). We have recently proposed a hierarchical oxidative stress model, which posits that incremental levels of oxidative stress initiate a series of cellular responses that vary according to the degree of GSH depletion (74). Thus, at the lowest level of oxidative stress (tier 1), Nrf2 release to the nucleus initiates transcriptional activation of the ARE and phase II enzyme expression (74). This response leads to cytoprotective and antioxidant effects, which could be effective for maintaining redox equilibrium. If, however, the level of oxidative stress exceeds tier 1 protection, the cellular response progresses to activating proinflammatory signaling pathways (tier 2), including NF-κB and MAPK cascades. These signaling pathways regulate cytokine, chemokine, and adhesion molecule expression. Further escalation of the level of oxidative stress to tier 3 leads to mitochondrial perturbation and PTP opening (74). This could initiate apoptosis and necrosis. Based on this hierarchical model, tier 1 effects could play an important role in the long term survival of memory T cells. This is compatible with the observation that aged T cells, especially the memory subset, exhibit increased phase II enzyme expression (Figs. 6 and 7) as well as increased intracellular thiol levels (Fig. 5). Increased phase II enzyme expression could be essential for protecting the long-lived memory cells against progressive mitochondrial dysfunction (Figs. 3 and 4).

Phase II enzymes exert cytoprotective, antioxidant, and anti-inflammatory effects (48–50, 75–80). For instance, HO-1 is an inducible heme oxygenase that is responsible for bilirubin production through heme catabolism (75). Bilirubin has potent antioxidant and anti-inflammatory effects. A variety of GST isotypes play a role in GSH-dependent detoxification of reactive electrophiles, such as genotoxic carcinogens (48). γ-GCLR is the regulatory subunit of γ-GCL, which catalyzes the rate-limiting step in GSH biosynthesis (49). SOD catalyzes the conversion of single electron-reduced molecular oxygen species to hydrogen peroxide. Different SOD isoforms vary in their metal binding affinities, subcellular distribution, and sensitivity to oxidative agents (76). GPx is a well-known selenoenzyme that catalyzes the reduction of harmful peroxides by GSH and protects cells against oxidative damage (50). NQO-1 protects cells against redox cycling chemicals that are involved in one-electron reductions, e.g., quinones and transition metals (77). Recently, NQO-1 has also been implicated in the generation of antioxidants, such as ubiquinones and vitamin E (77), and has been shown to be expressed in a variety of tissues that require a high level of antioxidant protection (78–80).

Phase II enzymes play an important role during aging, with data from various laboratories showing age-related changes in phase II enzyme expression, with some specificity with respect to tissue type, organelle, animal strain, and sex (81–87). For instance, HO-1 has been reported to increase in brain and liver tissues with aging (81, 82), whereas SOD and CAT activities were increased in the brain, and CAT and GPx were elevated in the liver of aged mice (83). Moreover, SOD, CAT, and GPx activities increase in different regions of the aged C57BL/6N brain (84). Some studies looking at erythrocytes have also described negative correlations between SOD activity and age, with CAT and GPx deviating in the opposite direction (85). Aging also leads to a decreased expression of the catalytic and modulatory subunits of the γ-GCL gene (86). It has been demonstrated that CAT and SOD activities undergo changes in the spleen and thymus of older animals (87). For instance, Bonzan et al. (87) reported that aging is associated with a marked decrease in the antioxidant defense capacity of spleen and a strong increase in SOD activity in the thymus and liver. In this communication we demonstrate for the first time that there is an increase in phase II enzyme expression in memory T lymphocytes with aging. Our data indicate that the $CD4^+$ memory cells express significantly higher HO-1, NQO-1, GPx, γ-GCLR, and CAT mRNA levels than naive T cells (Fig. 7).

Nrf2 is important for transcriptional activation of the ARE in combination with small Maf and AP-1 proteins. Under basal conditions, Keap I is responsible for sequestering Nrf2 in the cytosol (42, 54, 55). Keap I is also responsible for shuttling Nrf2 to the 26S proteosome, where it is rapidly degraded under basal conditions. However, under conditions of oxidative stress, Nrf2 is uncoupled from Keap I, leading to a prolonged Nrf2 half-life and accumulation in the nucleus. In addition to regulating Nrf2 abundance by this proteosomal mechanism, the transcription factor level is also dependent on mRNA expression (56, 57). Kwak et al. (57) showed that Nrf2 autoregulates its own expression through ARE-like *cis* elements in the promoter. The accompanying increase in Nrf2 synthesis could saturate the available Keap 1 binding sites, allowing for Nrf2 entry to the nucleus. Although it was not logistically feasible to study Nrf2 half-life due to low protein abundance, we demonstrated a significance increase in Nrf2 mRNA levels in memory compared with naive $CD4^+$ cells (Fig. 7*C*). We propose that this increase contributes to increased phase II mRNA expression in memory cells. This is consistent with the increased mRNA levels for HO-1, NQO-1, GPx, γ-GCLR, and CAT in these cells (Fig. 7*B*).

Decreased $\Delta\psi_m$ has been demonstrated in a variety of senescent cell types, including lymphocytes (14, 88). Cyclosporin A, an inhibitor of mitochondrial PTP, can restore the $\Delta\psi_m$ in $DiOC_6^{low}/HE^{low}$ cells (47), which corresponds to the phenotype of most memory T cells in old mice (Fig. 4*A*). Although the reason for this

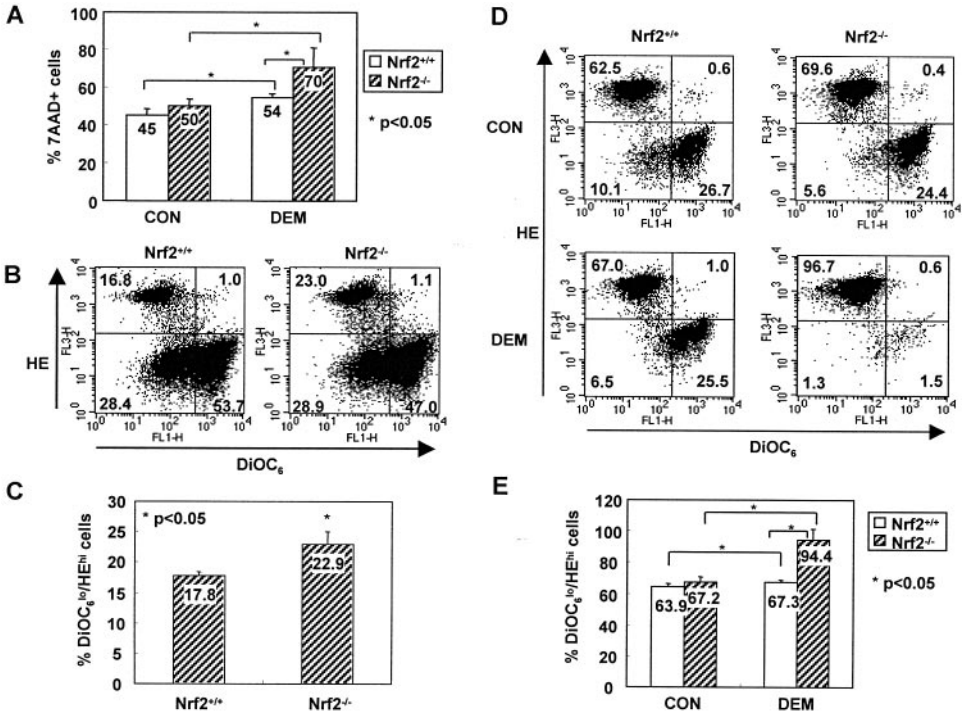

FIGURE 9. Nrf2 protects T cells against DEM-induced cell death and mitochondrial perturbation. *A*, Nylon-wool-purified splenic T cells from wild-type (*Nrf2*$^{+/+}$) and *Nrf2*-deficient (*Nrf2*$^{-/-}$) mice were cultured for 1 day with or without 0.2 μM DEM. The cells were stained with 7-AAD, followed by flow cytometric analysis. A comparison of the percentage of total apoptotic cells from the splenic T cells of *Nrf2*$^{+/+}$ and *Nrf2*$^{-/-}$ mice is shown. Data represent the mean $\pm$ SD of the percentage of dead cells ($n = 4$). *, $p < 0.05$, young vs old mice, or DEM vs control. *B* and *C*, Freshly isolated T cells were dual stained with $DiOC_6$ and HE as described in Fig. 4. *B*, Representative scattergram comparing total T cells from *Nrf2*$^{+/+}$ and *Nrf2*$^{-/-}$ mice. The number in each quadrant refers to the percentage of cells in that population. *C*, Mean $\pm$ SD, comparing the percentage of $DiOC_6^{low}/HE^{high}$ cells in *Nrf2*$^{+/+}$ mice with those in *Nrf2*$^{-/-}$ mice ($n = 4$/group). *, $p < 0.05$, *Nrf2*$^{+/+}$ vs *Nrf2*$^{-/-}$ mice. *D* and *E*, Splenic T cells were cultured for 1 day in the absence or the presence of 0.2 μM DEM. The cells were stained as described in *B*. A representative scattergram shows the percentage of cells in each quadrant. *E*, Statistical analysis of the percentage of $DiOC_6^{low}/HE^{high}$ cells (mean $\pm$ SD) in *Nrf2*$^{+/+}$ compared with *Nrf2*$^{-/-}$ mice ($n = 4$/group). *, $p < 0.05$, young vs old, or DEM vs control mice.

reversibility is not well understood, it is possible that this could be a regulated mitochondrial oxidative stress response. The PTP contains vicinal thiol groups that are sensitive to oxidative stress (29). The oxidation of these cysteine residues can be reversed by GSH and antioxidant enzymes, thereby regulating the extent to which mitochondrial dysfunction impacts cellular processes (Figs. 3 and 4). Because Nrf2 regulates these antioxidant defense pathways, this transcription factor could be important for memory T cell survival (Figs. 5 and 7). This was confirmed by the demonstration that *Nrf2* deficiency promotes T cell apoptosis, $\Delta\psi_m$ decline, and O_2^- generation in the presence of an oxidative stress (Fig. 9).

We show that *Nrf2* deficiency renders T cells more susceptible to mitochondrial perturbation and apoptosis in the presence of an exogenous oxidative stress stimulus. However, this difference is not significant in *Nrf2*-deficient mice under basal conditions (Fig. 9). It will be interesting to determine whether the oxidative stress effects of natural aging have the same effects in these animals. Unfortunately, we did not have access to aged *Nrf2*$^{-/-}$ animals to perform this study. Moreover, performance of these experiments could be difficult due to the propensity of aged *Nrf2*$^{-/-}$ mice to develop a lupus-like disorder with accumulation of autoreactive B cells in the spleen (89–91). Nonetheless, the use of younger *Nrf2* knockout animals is helpful for proof-of-principle testing to demonstrate the role of this transcription factor in apoptosis and mitochondrial dysfunction. DEM treatment leads to an increased rate of apoptosis and mitochondrial dysfunction in *Nrf2*$^{-/-}$ T cells (Fig. 9). This contribution of Nrf2 to the generation of apoptosis in young mice is one of many factors that regulate cell viability, including Bcl-2.

In summary, we show that memory T cells differ from naive T cells in the degree of mitochondrial dysfunction and expression of antioxidant defense. Nrf2-mediated expression of phase II antioxidant enzymes protects memory T cells from mitochondrial dysfunction. This mechanism could contribute, at least in part, to the accumulation of memory T cells during aging. Detailed additional studies to delineate the role of antioxidant defense pathways in Ag-specific immune responses, including activation-induced apoptosis, are in progress.

Acknowledgments

Flow cytometry was performed at the University of California-Los Angeles Jonsson Comprehensive Cancer Center and the Center for AIDS Research Flow Cytometry Core Facility, University of California-Los Angeles AIDS Institute, and the David Geffen School of Medicine at University of California-Los Angeles. We thank Dr. Kenneth Dorshkind (University of California-Los Angeles, CA) for providing spleens of young and old B6 mice, and Dr. Jamie Lee (Mayo Clinic, Scottsdale, AZ) for breeding the *Nrf2*$^{-/-}$ mice onto a C57BL/6 background. We thank Ndaisha Slaughter for technical assistance.

Disclosures

The authors have no financial conflict of interest.

References

1. Thoman, M. L., and W. O. Weigle. 1989. The cellular and subcellular bases of immunosenescence. *Adv. Immunol.* 46: 221–261.
2. Grubeck-Loebenstein, B. 1997. Changes in the aging immune system. *Biologicals* 25: 205–208.
3. Hodes, R. J. 1995. Molecular alterations in the aging immune system. *J. Exp. Med.* 182: 1–3.
4. Miller, R. A. 2000. Effect of aging on T lymphocyte activation. *Vaccine* 18: 1654–1660.
5. Song, L., Y. H. Kim, R. K. Chopra, J. J. Proust, J. E. Nagel, A. A. Nordin, and W. H. Adler. 1993. Age-related effects in T cell activation and proliferation. *Exp. Gerontol.* 28: 313–321.
6. Hobbs, M. V., W. O. Weigle, D. J. Noonan, B. E. Torbett, R. J. McEvilly, R. J. Koch, G. J. Cardenas, and D. N. Ernst. 1993. Patterns of cytokine gene expression by $CD4^+$ T cells from young and old mice. *J. Immunol.* 150: 3602–3614.
7. Engwerda, C. R., B. S. Fox, and B. S. Handwerger. 1996. Cytokine production by T lymphocytes from young and aged mice. *J. Immunol.* 156: 3621–3630.
8. Tanchot, C., M. M. Rosado, F. Agenes, A. A. Freitas, and B. Rocha. 1997. Lymphocyte homeostasis. *Semin. Immunol.* 9: 331–337.
9. Sprent, J. 1993. Lifespans of naive, memory and effector lymphocytes. *Curr. Opin. Immunol.* 5: 433–438.
10. Fernandes, G., J. T. Venkatraman, A. Turturro, V. G. Attwood, and R. W. Hart. 1997. Effect of food restriction on life span and immune functions in long-lived Fischer-344 × Brown Norway F_1 rats. *J. Clin. Immunol.* 17: 85–95.
11. Harman, D. 1956. Aging: a theory based on free radical and radiation chemistry. *J. Gerontol.* 11: 298–300.
12. Yu, B. P. 1996. Aging and oxidative stress: modulation by dietary restriction. *Free Radic. Biol. Med.* 21: 651–668.
13. De la Fuente, M. 2002. Effects of antioxidants on immune system ageing. *Eur. J. Clin. Nutr.* 56:S5–S8.
14. Sugrue, M. M., and W. G. Tatton. 2001. Mitochondrial membrane potential in aging cells. *Biol. Signals Recept.* 10: 176–188.
15. Sastre, J., F, V. Pallardo, and J. Vina. 2000. Mitochondrial oxidative stress plays a key role in aging and apoptosis. *IUBMB Life* 49: 427–435.
16. Kroemer, G., B. Dallaporta, and M. Resche-Rigon. 1998. The mitochondrial death/life regulator in apoptosis and necrosis. *Annu. Rev. Physiol.* 60: 619–642.
17. Bossy-Wetzel, E., M. J. Barsoum, A. Godzik, R. Schwarzenbacher, and S. A. Lipton. 2003. Mitochondrial fission in apoptosis, neurodegeneration and aging. *Curr. Opin. Cell Biol.* 15: 706–716.
18. Sainz, R. M., J. C. Mayo, R. J. Reiter, D. X. Tan, and C. Rodriguez. 2003. Apoptosis in primary lymphoid organs with aging. *Microsc. Res. Tech.* 62: 524–539.
19. Zhang, J. H., Y. Zhang, and B. Herman. 2003. Caspases, apoptosis and aging. *Ageing Res. Rev.* 2: 357–366.
20. Pollack, M., S. Phaneuf, A. Dirks, and C. Leeuwenburgh. 2002. The role of apoptosis in the normal aging brain, skeletal muscle, and heart. *Ann. NY Acad. Sci.* 959: 93–107.
21. Zhang, X., H. Fujii, H. Kishimoto, E. LeRoy, C. D. Surh, and J. Sprent. 2002. Aging leads to disturbed homeostasis of memory phenotype $CD8^+$ cells. *J. Exp. Med.* 195: 283–293.
22. Aggarwal, S., and S. Gupta. 1998. Increased apoptosis of T cell subsets in aging humans: altered expression of Fas (CD95), Fas ligand, Bcl-2, and Bax. *J. Immunol.* 160: 1627–1637.
23. Monti, D., S. Salvioli, M. Capri, W. Malorni, E. Straface, A. Cossarizza, B. Botti, M. Piacentini, G. Baggio, C. Barbi, et al. 2000. Decreased susceptibility to oxidative stress-induced apoptosis of peripheral blood mononuclear cells from healthy elderly and centenarians. *Mech. Ageing Dev.* 121: 239–250.
24. Phelouzat, M. A., A. Arbogast, T. Laforge, R. A. Quadri, and J. J. Proust. 1996. Excessive apoptosis of mature T lymphocytes is a characteristic feature of human immune senescence. *Mech. Ageing Dev.* 88: 25–38.
25. Dennett, N. S., R. N. Barcia, and J. D. McLeod. 2002. Age associated decline in CD25 and CD28 expression correlate with an increased susceptibility to CD95 mediated apoptosis in T cells. *Exp. Gerontol.* 37: 271–283.
26. Halliwell, B., and J. M. C. Gutteridge. 1999. *Free Radicals in Biology and Medicine*. Oxford University Press, Oxford.
27. Griffiths, H. R. 2000. Antioxidants and protein oxidation. *Free Radic. Res.* 33: S47–S58.
28. Hayes, J. D., and L. I. McLellan. 1999. Glutathione and glutathione-dependent enzymes represent a coordinately regulated defence against oxidative stress. *Free Radic. Res.* 31: 273–300.
29. Costantini, P., B. V. Chernyak, V. Petronilli, and P. Bernardi. 1996. Modulation of the mitochondrial permeability transition pore by pyridine nucleotides and dithiol oxidation at two separate sites. *J. Biol. Chem.* 271: 6746–6751.
30. Fernandez-Checa, J. C., C. Garcia-Ruiz, A. Colell, A. Morales, M. Mari, M. Miranda, and E. Ardite. 1998. Oxidative stress: role of mitochondria and protection by glutathione. *Biofactors* 8: 7–11.
31. Nguyen, T., P. J. Sherratt, and C. B. Pickett. 2003. Regulatory mechanisms controlling gene expression mediated by the antioxidant response element. *Annu. Rev. Pharmacol. Toxicol.* 43: 233–260.
32. Talalay, P. 2000. Chemoprotection against cancer by induction of phase 2 enzymes. *Biofactors* 12: 5–11.
33. Lee, J. M., A. Y. Shih, T. H. Murphy, and J. A. Johnson. 2003. NF-E2-related factor-2 mediates neuroprotection against mitochondrial complex I inhibitors and increased concentrations of intracellular calcium in primary cortical neurons. *J. Biol. Chem.* 278: 37948–37956.
34. Chan, K., and Y. W. Kan. 1997. Nrf2 is essential for protection against acute pulmonary injury in mice. *Proc. Natl. Acad. Sci. USA* 96: 12731–12736.
35. Miltenyi, S., W. Muller, W. Weichel, and A. Radbruch. 1990. High gradient magnetic cell separation with MACS. *Cytometry* 11: 231–238.
36. Schmid, I., W. J. Krall, C. H. Uittenbogaart, J. Braun, and J. V. Giorgi. 1992. Dead cell discrimination with 7-amino-actinomycin D in combination with dual color immunofluorescence in single laser flow cytometry. *Cytometry* 13: 204–208.
37. Donner, K. J., K. M. Becker, B. D. Hissong, and S. Ansar Ahmed. 1999. Comparison of multiple assays for kinetic detection of apoptosis in thymocytes exposed to dexamethasone or diethylstilbesterol. *Cytometry* 35: 80–90.
38. Gogal, R. M., Jr., B. J. Smith, J. Kalnitsky, and S. D. Holladay. 2000. Analysis of apoptosis of lymphoid cells in fish exposed to immunotoxic compounds. *Cytometry* 39: 310–318.
39. Schmid, I., C. H. Uittenbogaart, B. Keld, and J. V. Giorgi. 1994. A rapid method for measuring apoptosis and dual-color immunofluorescence by single laser flow cytometry. *J. Immunol. Methods* 170: 145–157.
40. Roederer, M., F. J. Staal, H. Osada, L. A. Herzenberg, and L. A. Herzenberg. 1991. CD4 and CD8 T cells with high intracellular glutathione levels are selectively lost as the HIV infection progresses. *Int. Immunol.* 3: 933–937.
41. Hedley, D. W., and S. Chow. 1994. Evaluation of methods for measuring cellular glutathione content using flow cytometry. *Cytometry* 15: 349–358.
42. Li, N., J. Alam, M. I. Venkatesan, A. Eiguren-Fernandez, D. Schmitz, E. Di Stefano, N. Slaughter, E. Killeen, X. Wang, A. Huang, et al. 2004. Nrf2 is a key transcription factor that regulates antioxidant defense in macrophages and epithelial cells: protecting against the proinflammatory and oxidizing effects of diesel exhaust chemicals. *J. Immunol.* 173: 3467–3481.
43. Li, N., M. I. Venkatesan, A. Miguel, R. Kaplan, C. Gujuluva, J. Alam, and A. Nel. 2000. Induction of heme oxygenase-1 expression in macrophages by diesel exhaust particle chemicals and quinones via the antioxidant-responsive element. *J. Immunol.* 165: 3393–3401.
44. Vella, A. T., S. Dow, T. A. Potter, J. Kappler, and P. Marrack. 1998. Cytokine-induced survival of activated T cells in vitro and in vivo. *Proc. Natl. Acad. Sci. USA* 95: 3810–3815.
45. King, L. B., and J. D. Ashwell. 1993. Signaling for death of lymphoid cells. *Curr. Opin. Immunol.* 5: 368–373.
46. Rathmell, J. C., and C. B. Thompson. 2002. Pathways of apoptosis in lymphocyte development, homeostasis, and disease. *Cell* 109: S97–S107.
47. Zamzami, N., P. Marchetti, M. Castedo, D. Decaudin, A. Macho, T. Hirsch, S. A. Susin, P. X. Petit, B. Mignotte, and G. Kroemer. 1995. Sequential reduction of mitochondrial transmembrane potential and generation of reactive oxygen species in early programmed cell death. *J. Exp. Med.* 182: 367–377.
48. Hayes, J. D., and R. C. Strange. 1995. Potential contribution of the glutathione *S*-transferase supergene family to resistance to oxidative stress. *Free Radic. Res.* 22: 193–207.
49. Griffith, O. W., and R. T. Mulcahy. 1999. The enzymes of glutathione synthesis: γ-glutamylcysteine synthetase. *Adv. Enzymol. Relat. Areas Mol. Biol.* 73: 209–267.
50. Miyamoto, Y., Y. H. Koh, Y. S. Park, N. Fujiwara, H. Sakiyama, Y. Misonou, T. Ookawara, K. Suzuki, K. Honke, and N. Taniguchi. 2003. Oxidative stress caused by inactivation of glutathione peroxidase and adaptive responses. *Biol. Chem.* 384: 567–574.
51. Owuor, E. D., and A. T. Kong. 2002. Antioxidants and oxidants regulated signal transduction pathway. *Biochem. Pharmacol.* 64: 765–770.
52. Thimmulappa, R. K., K. H. Mai, S. Srisuma, T. W. Kensler, M. Yamamoto, and S. Biswal. 2002. Identification of Nrf2-mediated genes induced by the chemoprevented agent sulforaphane by oligonucleotide microarray. *Cancer Res.* 62: 5196–5203.
53. Morito, N., K. Yoh, K. Itoh, A. Hirayama, A. Koyama, M. Yamamoto, and S. Takahashi. 2003. Nrf2 regulates the sensitivity of death receptor signals by affecting intracellular glutathione levels. *Oncogene* 22: 9275–9281.
54. Stewart, D., E. Killeen, R. Naquin, S. Alam, and J. Alam. 2003. Degradation of transcription factor Nrf2 via the ubiquitin-proteasome pathway and stabilization by cadmium. *J. Biol. Chem.* 278: 2396–2402.
55. McMahon, M., K. Itoh, M. Yamamoto, and J. D. Hayes. 2003. Keap1-dependent proteasomal degradation of transcription factor Nrf2 contributes to the negative regulation of antioxidant response element-driven gene expression. *J. Biol. Chem.* 278: 21592–21600.
56. Cho, H. Y., A. E. Jedlicka, S. P. Reddy, T. W. Kensler, M. Yamamoto, L. Y. Zhang, and S. R. Kleeberger. 2002. Role of NRF2 in protection against hyperoxic lung injury in mice. *Am. J. Respir. Cell Mol. Biol.* 26: 175–182.
57. Kwak, M.-K., K. Itoh, M. Yamamoto, and T. W. Kensler. 2002. Enhanced expression of the transcription factor Nrf2 by cancer chemopreventive agents: role of antioxidant response element-like sequences in the *nrf2* promoter. *Mol. Cell. Biol.* 22: 2883–2892.
58. van Zandwijk, N. 1995. *N*-acetylcysteine (NAC) and glutathione (GSH): antioxidant and chemopreventive properties, with special reference to lung cancer. *J. Cell Biochem.* 22(Suppl.): 24–32.
59. De Rosa, S. C., M. D. Zaretsky, J. G. Dubs, M. Roederer, M. Anderson, A. Green, D. Mitra, N. Watanabe, H. Nakamura, I. Tjioe, et al. 2000. *N*-acetylcysteine replenishes glutathione in HIV infection. *Eur. J. Clin. Invest.* 30: 915–929.
60. Ghezzi, P., B. Romines, M. Fratelli, I. Eberini, E. Gianazza, S. Casagrande, T. Laragione, M. Mengozzi, L. A. Herzenberg, and L. A. Herzenberg. 2002. Protein glutathionylation: coupling and uncoupling of glutathione to protein thiol groups in lymphocytes under oxidative stress and HIV infection. *Mol. Immunol.* 38: 773–780.

61. Gil, L., G. Martinez, I. Gonzalez, A. Tarinas, A. Alvarez, A. Giuliani, R. Molina, R. Tapanes, J. Perez, and O. S. Leon. 2003. Contribution to characterization of oxidative stress in HIV/AIDS patients. *Pharmacol. Res.* 47: 217–224.
62. Repetto, M., C. Reides, M. L. Gomez Carretero, M. Costa, G. Griemberg, and S. Llesuy. 1996. Oxidative stress in blood of HIV infected patients. *Clin. Chim. Acta* 255: 107–117.
63. Israel, N., and M. A. Gougerot-Pocidalo. 1997. Oxidative stress in human immunodeficiency virus infection. *Cell. Mol. Life Sci.* 53: 864–870.
64. Dobmeyer, T. S., S. Findhammer, J. M. Dobmeyer, S. A. Klein, B. Raffel, D. Hoelzer, E. B. Helm, D. Kabelitz, and R. Rossol. 1997. Ex vivo induction of apoptosis in lymphocytes is mediated by oxidative stress: role for lymphocyte loss in HIV infection. *Free Radic. Biol. Med.* 22: 775–785.
65. Marmor, M., P. Alcabes, S. Titus, K. Frenkel, K. Krasinski, A. Penn, and R. W. Pero. 1997. Low serum thiol levels predict shorter times-to-death among HIV-infected injecting drug users. *AIDS* 11: 1389–1393.
66. Herzenberg, L. A., S. C. De Rosa, J. G. Dubs, M. Roederer, M. T. Anderson, S. W. Ela, S. C. Deresinski, and L. A. Herzenberg. 1997. Glutathione deficiency is associated with impaired survival in HIV disease. *Proc. Natl. Acad. Sci. USA* 94: 1967–1972.
67. Sun, D., A. Krishnan, J. Su, R. Lawrence, K. Zaman, and G. Fernandes. 2004. Regulation of immune function by calorie restriction and cyclophosphamide treatment in lupus-prone NZB/NZW F_1 mice. *Cell. Immunol.* 228: 54–65.
68. Pahlavani, M. A. 2004. Influence of caloric restriction on aging immune system. *J. Nutr. Health Aging* 8: 38–47.
69. Weindruch, R. 1996. Caloric restriction and aging. *Sci. Am.* 274: 46–52.
70. Lass, A., B. H. Sohal, R. Weindruch, M. J. Forster, and R. S. Sohal. 1998. Caloric restriction prevents age-associated accrual of oxidative damage to mouse skeletal muscle mitochondria. *Free Radic. Biol. Med.* 25: 1089–1097.
71. Lee, C. M., L. E. Aspnes, S. S. Chung, R. Weindruch, and J. M. Aiken. 1998. Influences of caloric restriction on age-associated skeletal muscle fiber characteristics and mitochondrial changes in rats and mice. *Ann. NY Acad. Sci.* 854: 182–191.
72. Dirks, A. J., and C. Leeuwenburgh. 2004. Aging and lifelong calorie restriction result in adaptations of skeletal muscle apoptosis repressor, apoptosis-inducing factor, X-linked inhibitor of apoptosis, caspase-3, and caspase-12. *Free Radic. Biol. Med.* 36: 27–39.
73. Yoon, S. O., C. H. Yun, and A. S. Chung. 2002. Dose effect of oxidative stress on signal transduction in aging. *Mech. Ageing Dev.* 123: 1597–1604.
74. Xiao, G. G., M. Wang, N. Li, J. A. Loo, and A. E. Nel. 2003. Use of proteomics to demonstrate a hierarchical oxidative stress response to diesel exhaust particle chemicals in a macrophage cell line. *J. Biol. Chem.* 278: 50781–50790.
75. Bauer, M., and I. Bauer. 2002. Heme oxygenase-1: redox regulation and role in the hepatic response to oxidative stress. *Antioxid. Redox Signal.* 4: 749–758.
76. Culotta, V. C. 2000. Superoxide dismutase, oxidative stress, and cell metabolism. *Curr. Top. Cell. Regul.* 36: 117–132.
77. Ross, D., J. K. Kepa, S. L. Winski, H. D. Beall, A. Anwar, and D. Siegel D. 2000. NAD(P)H:quinone oxidoreductase 1 (NQO1): chemoprotection, bioactivation, gene regulation and genetic polymorphisms. *Chem. Biol. Interact.* 129: 77–97.
78. Siegel, D., W. A. Franklin, and D. Ross. 1998. Immunohistochemical detection of NAD(P)H:quinone oxidoreductase in human lung and lung tumors. *Clin. Cancer Res.* 4: 2065–2070.
79. Schelonka, L. P., D. Siegel, M. W. Wilson, A. Meininger, and D. Ross. 2000. Immunohistochemical localization of NQO1 in epithelial dysplasia and neoplasia and in donor eyes. *Invest. Ophthalmol. Vis. Sci.* 41: 1617–1622.
80. Moran, J. L., D. Siegel, and D. Ross. 1999. A potential mechanism underlying the increased susceptibility of individuals with a polymorphism in NAD(P)H:quinone oxidoreductase 1 (NQO1) to benzene toxicity. *Proc. Natl. Acad. Sci. USA* 96: 8150–8155.
81. Hirose, W., K. Ikematsu, and R. Tsuda. 2003. Age-associated increases in heme oxygenase-1 and ferritin immunoreactivity in the autopsied brain. *Leg. Med. (Tokyo)* 5(Suppl.): S360–S366.
82. Lavrovsky, Y., C. S. Song, B. Chatterjee, and A. K. Roy. 2000. Age-dependent increase of heme oxygenase-1 gene expression in the liver mediated by NFκB. *Mech. Ageing Dev.* 114: 49–60.
83. Wozniak, A., G. Drewa, B. Wozniak, and D. O. Schachtschabel. 2004. Activity of antioxidant enzymes and concentration of lipid peroxidation products in selected tissues of mice of different ages, both healthy and melanoma-bearing. *Z. Gerontol. Geriatr.* 37: 184–189.
84. Hussain, S., W. Slikker, Jr., and S. F. Ali. 1995. Age-related changes in antioxidant enzymes, superoxide dismutase, catalase, glutathione peroxidase and glutathione in different regions of mouse brain. *Int. J. Dev. Neurosci.* 13: 811–817.
85. Inal, M. E., G. Kanbak, and E. Sunal. 2001. Antioxidant enzyme activities and malondialdehyde levels related to aging. *Clin. Chim. Acta* 305: 75–80.
86. Suh, J. H., S. V. Shenvi, B. M. Dixon, H. Liu, A. K. Jaiswal, R. M. Liu, and T. M. Hagen. 2004. Decline in transcriptional activity of Nrf2 causes age-related loss of glutathione synthesis, which is reversible with lipoic acid. *Proc. Natl. Acad. Sci. USA* 101: 3381–3386.
87. Bolzan, A. D., O. A. Brown, R. G. Goya, and M. S. Bianchi. 1995. Hormonal modulation of antioxidant enzyme activities in young and old rats. *Exp. Gerontol.* 30: 169–175.
88. Rottenberg, H., and S. Wu. 1997. Mitochondrial dysfunction in lymphocytes from old mice: enhanced activation of the permeability transition. *Biochem. Biophys. Res. Commun.* 240: 68–74.
89. Lee, J., K. Chan, Y. W. Kan, and J. A. Johnson. 2004. Targeted disruption of Nrf2 causes regenerative immune-mediated hemolytic anemia. *Proc. Natl. Acad. Sci. USA* 101: 9751–9756.
90. Li, J., T. D. Stein, and J. A. Johnson. 2004. Genetic dissection of systemic autoimmune disease in Nrf2-deficient mice. *Physiol. Genomics* 18: 261–272.
91. Yoh, K., K. Itoh, A. Enomoto, A. Hirayama, N. Yamaguchi, M. Kobayashi, N. Morito, A. Koyama, M. Yamatomo, and S. Takahashi. 2001. Nrf2-deficient female mice develop lupus-like autoimmune nephritis. 2001. *Kidney Int.* 60: 1343–1353.